Use of sewage sludge combustion ash and gasification ash for high-temperature desulphurization of different gas streams

N. Gil-Lalaguna *, J. L. Sánchez, M. B. Murillo, G. Gea

Thermo-chemical Processes Group, Aragón Institute of Engineering Research (I3A), Universidad de Zaragoza, c/ Mariano Esquillor s/n., 50018, Zaragoza, Spain.

* Corresponding Author Tel: +34976762224 e-mail: noemigil@unizar.es

Abstract

Due to its metal content, sewage sludge ash appears as a potential sorbent material for H_2S removal at high temperature. The desulphurization ability of the solid by-products of combustion and gasification of sewage sludge has been evaluated in this work. Ash characterization results revealed that metal fraction in sewage sludge did not remained completely inert during the combustion and gasification processes. Iron content was lower in the gasification ash and X-ray patterns showed different crystalline phases in the solids: Fe_2O_3 in the combustion ash and Fe_3O_4 in the gasification ash. These differences resulted in a lower sulphur capture capacity of the gasification ash. Desulphurization tests were carried out in a lab-scale fixed bed reactor operating at 600-800 ºC. Different gases containing 5000 ppmv H_2S (H_2S/N_2 mixture and synthetic gasification gas) were used. The H_2S breakthrough curves were negatively affected by the reducing atmosphere created by the gasification gas and by the presence of steam in the reaction medium. However, H_2S breakthrough curves alone do not provide enough information to evaluate the sulphur capture capacity of the sorbent materials. Ultimate analyses of the spent solid samples showed that the total amount of H_2S removed from the gas was only partially captured in the ash. Thermodynamic data pointed to a significant fraction of sulphur forming part of other gases, such as SO_2. In the best

operating conditions, an outlet gas with less than 100 ppmv of H_2S was obtained during 300 min, thus resulting in a sulphur loading of 63 mg $S \cdot g^{-1}_{ash}$. This experimental sulphur content was 39% lower than the maximum theoretical value predicted by equilibrium simulations.

Keywords: H_2S removal; hot gas cleaning; sewage sludge; combustion ash; gasification ash.

1. Introduction

Sewage sludge has become an increasingly important residue needing effective management. Due to the organic nature of sewage sludge, thermal processes such as pyrolysis, gasification or combustion have attracted considerable scientific interest as a potential route to its energy valorization [1-3]. However, as occurs in most thermo-chemical treatments of wastes and solid fuels, various impurities are found in the products of interest deriving from these processes, which significantly limits their final uses. One of these impurities is H_2S, present in the gaseous products of both the pyrolysis and the gasification of sewage sludge due to its initial content of sulphur compounds [4]. As is well known, H_2S emissions to the atmosphere (or SO_2 emissions in the case of burning a H_2S-containing gas) entail environmental problems related to acid rain. In addition, the presence of H_2S in the gas leads to operational problems such as corrosion in pipes, engines or turbines, as well as the deactivation of the common catalysts used for tar cracking and gas reforming after gasification processes [5].

Several low and high temperature processes for the elimination of H_2S from products or off-gases have been described and developed at various stages. Wet scrubbing with selected solvents has been a widely used low-temperature process in the chemical process industry [6]. The use of activated carbons for H_2S removal at low

temperature has also been extensively studied [7-9]. Given the combination of their unique surface features (high specific surface and pore volume) and surface chemistry (improved by the addition of functional groups or by its metallic content), activated carbon-based materials have been proved to work efficiently as adsorbents of sulphur-containing species such as H_2S, SO_2 or methyl mercaptans from the gas phase. As a result of surface reactions, H_2S can be oxidized to either sulphur or SO_2 [8]. Activated carbons of different characteristics have also been prepared from sewage sludge pyrolysis or carbonization [10-13], obtaining pollutant removal results comparable to those corresponding to commercial catalytic activated carbons [13].

On the other hand, high temperature desulphurization processes are advantageous from an energy standpoint as a result of the elimination of gas cooling and the associated heat exchangers [14]. Different studies on the use of metal oxide based sorbents for hot gas desulphurization can be found in the literature [14-20]. Zinc, manganese, copper, iron, rare earth, and calcium sorbents are among the most promising and most extensively studied [14, 15]. Typically, metal oxides are converted to sulphides during a sulphur loading stage under reducing hot gas conditions. After sulphidation, the spent metal sulphides can be regenerated back to metal oxides by using oxygen, steam, SO_2 or a combination of these [14].

Ash residues derived from thermo-chemical processes are known to contain metal oxides in different proportions, so its use as sorbent materials for H_2S removal from hot gases could be an attractive alternative due to its low cost. This is the case of sewage sludge ash, in which this work focuses. An integrated process could be proposed to remove the H_2S produced during thermo-chemical treatment of sewage sludge by using the own ash resulting from these processes in a downstream cleaning stage. The desulphurization capacity of the solid by-products derived from the combustion and

gasification of sewage sludge has been evaluated in this work. Desulphurization tests were carried out in a lab-scale fixed bed reactor and the effects of temperature, type of sewage sludge ash, presence of steam and type of H_2S-containing gas were studied, thus extending an earlier work performed by our group [20].

2. Materials and methods

2.1. Sewage sludge ash

The raw material used to obtain the ash samples was anaerobically digested and thermally dried sewage sludge. Sewage sludge combustion was performed under air atmosphere in a heating muffle furnace at 900 ºC (heating rate of 20 ºC·min^{-1}) during two hours. The sewage sludge gasification ash was obtained in a previous gasification study performed in a lab-scale fluidized bed reactor at 850 ºC, using a mixture of steam and air as gasifying agent (H_2O/O_2 molar ratio = 1) [4].

The fresh ash samples were characterized by various techniques. Ultimate analyses were performed using a Leco TruSpec Micro elemental analyzer. The textural properties such as the BET surface area and the average pore size and volume (BJH method) were calculated from N_2 physisorption isotherms (BET volumetric method) using a Micromeritics TriStar II 3000 analyzer. The N_2 adsorption-desorption isotherms were obtained at -196 ºC and room temperature, respectively, over the whole range of relative pressures. The samples were previously degasified at 200 ºC during 8 h in a N_2 flow. Powder X-ray diffraction (XRD) patterns of the fresh samples were acquired with a D-Max Rigaku diffractometer equipped with a copper anode (voltage of 40 kV and current of 80 mA). The measurements were completed in the Bragg's angle (2θ) range from 5º to 95º, using a scanning rate of 0.03º·s^{-1}. Phases present in the solid samples were defined according to the JCPDS-International Centre for Diffraction Data 2000

database. Lastly, metal content in the ash samples was analyzed by inductively coupled plasma combined with optical emission spectroscopy (ICP-OES), using a Thermo Elemental IRIS Intrepid ICP-OES spectrometer. The samples were dissolved by microwave-assisted acid digestion in a CEM MARS microwave reaction system.

2.2. Experimental setup and operating conditions

The desulphurization tests were performed at atmospheric pressure in a fixed-bed quartz tubular reactor of 1.2 cm internal diameter and 40 cm length. A schematic diagram of the installation used for the desulphurization tests is shown in Fig. 1. The reactor was packed with 1 g of the solid material (combustion ash or gasification ash), which was supported on a fiberglass fleece located 18.5 cm from the top of the reactor. A K-type thermocouple was located in the middle of the solid bed and the reactor was electrically heated to the final temperature (600, 700 or 800 ºC). The flow rate of the H_2S-containing gas was adjusted to 50 $mL_{STP} \cdot min^{-1}$ (STP: standard conditions of temperature and pressure at 0 ºC and 1 atm) by means of a previously calibrated mass flow controller. Two different inlet gases containing 5000 ppmv H_2S were used to evaluate the effect of the gas components on the desulphurization process: (i) a gas mixture only containing H_2S and N_2 and (ii) a synthetic gasification gas, similar to the dry product gas of sewage sludge gasification [4]. Table 1 shows the composition of both gas mixtures. On the one hand, the H_2S/N_2 mixture allows the assessment of the desulphurization process without involving any interference from other gases. On the other hand, the synthetic gasification gas simulates more real conditions for the H_2S removal from a gasification gas. Steam was also added in some tests in order to evaluate its effect on the desulphurization ability of the solids. The required flow of liquid water (0-1 $g \cdot h^{-1}$) was accurately adjusted by a HPLC pump and was evaporated before entering the reactor. Steam concentration in the gas entering the reactor varied from 0 to

30 vol. %, which led to a H_2O/H_2S mass ratio varying from 0 to 45 g H_2O/g H_2S. The weight hourly space velocity during the experiments ranged between 3.7 h^{-1} and 4.7 h^{-1} depending on the steam feed rate. The gas-solid contact time was chosen after preliminary experiments and based on earlier studies [20].

The reactor containing the ash sample was flushed with a N_2 flow while heating. The experiment started when the desired temperature was reached in the solid bed. Just then the N_2 flow was replaced by the synthetic gasification gas or by the H_2S/N_2 mixture. The composition of the outlet gas was continuously analyzed during the experiments by means of an Agilent Micro-GC 3000 (sample injection every four minutes). The H_2S outlet flow ($mL_{STP} \cdot min^{-1}$) was calculated from the gas composition data taking the nitrogen of the gas mixture as an internal standard. The evolution of the H_2S outlet flow with time is depicted in the H_2S breakthrough curves. Initially, the established time for the experiments was two hours, but reaction time was extended in some cases to 240 or 390 min (Table 2) in order to reach the H_2S breakthrough time.

After the desulphurization tests, sulphur content in the ash samples was determined with a Leco TruSpec Micro elemental analyzer. Furthermore, one of the ash samples was morphologically and chemically characterized by scanning electron microscopy combined with energy dispersive X-ray spectroscopy (SEM/EDX) and by X-ray photoelectron spectroscopy (XPS). A FEI Inspect F50 microscope was used for the SEM/EDX analysis. External metal coating was not applied to the solid sample. The back-scattered electron imaging mode was used in the EDX analysis (acquisition time of 1 min). The XPS measurements were performed with a Kratos AXIS ultra DLD spectrometer by using monochromatic Al Kα (1486.6 eV) X-ray source and a chamber pressure of around $3 \cdot 10^{-8}$ Pa. The quantification of the XPS spectra was carried out with

the help of the CasaXPS software and the spectra were deconvoluted by applying Gaussian-Lorentzian line-shapes with Shirley-type background.

Table 2 summarizes the operating conditions for the desulphurization tests. In summary, the operating factors studied were the following: bed temperature (600-800 ºC), H_2O/H_2S mass ratio in the inlet gas (0-45 g/g), type of sewage sludge ash (combustion ash or gasification ash) and type of H_2S-containing gas (H_2S/N_2 mixture or synthetic gasification gas). Blank tests (with no bed material) were also performed at the different temperatures and gas atmospheres in order to assess any side effect of the experimental setup caused, for example, by the reaction of H_2S with the hot metal parts (made of steel) at the reactor inlet and outlet. On the other hand, experimental variability was evaluated through three replicates performed when feeding the H_2S/N_2 mixture and operating in the intermediate values of temperature (700 ºC) and H_2O/H_2S mass ratio (22.5 g/g). The impact of the studied factors was statistically analyzed by means of analysis of variance ANOVA (confidence level of 95% for the F-distribution). Design-Expert® 7 software (from Stat-Ease, Inc.) was used for this purpose. The use of coded levels for the factors (-1 for the lower limits and +1 for the upper limits) in the ANOVA analysis enables an easy identification of the term with the greatest influence: the higher the absolute value of the coefficient, the more influential the factor. Although the type of sewage sludge ash is not a numerical factor, a coded value of -1 was assigned to the combustion ash and +1 to the gasification ash in order to obtain comparable coefficients from the ANOVA analysis.

The desulphurization tests performed at the laboratory were also theoretically simulated to determine the maximum amount of H_2S that could be removed from the gas from a thermodynamic point of view. HSC Chemistry® 6.1 software was used for this purpose. This software uses the Gibbs energy minimization method to calculate the

amounts of products at equilibrium in isothermal and isobaric conditions. The reaction system must be specified for the calculations.

3. Results and discussion

The characterization results of the fresh ash samples are presented in subsection 3.1. After that, desulphurization performance results are shown and discussed in two different subsections according to the gas mixture used (3.2 and 3.3). The H_2S breakthrough curves and the sulphur content in the solid samples (expected and measured data) are the main results evaluated.

3.1. Characterization of the fresh ash samples

Table 3 summarizes the characterization results of the fresh ash samples resulting from combustion and gasification of sewage sludge. Both solids contained a small fraction of sulphur and some amount of carbon was also present in the gasification ash (around 3 wt. %). The surface properties of sewage sludge ash are not good enough for its use as an adsorbent material, but its desulphurization potential is based on its metallic content. The main metallic elements detected by ICP-OES were Fe, Si, Ca and Al. According to the thermodynamic study reported by Westmoreland and Harrison [21] concerning the desulphurization potential of different metal oxides, Ca and Fe oxides are able to react with H_2S to form metal sulphides, so both ash samples are potential sulphur sorbents. Some differences were found in the metal content of the solids, which might indicate that the ash fraction of sewage sludge did not remained completely inert during the combustion and gasification processes. Heterogeneity of sewage sludge may also explain these differences. Particularly striking is the case of Fe content which was much lower in the gasification ash. Part of the Fe content in the raw sewage sludge could be in the form of iron chloride ($FeCl_3$) as a result of the use of this compound as a

coagulant agent in the wastewater treatment plant. During combustion, the excess oxygen appears to favor the retention of Fe in the ash in the oxide form. However, part of the Fe content could remain as $FeCl_3$ during the gasification process due to the reduced presence of oxygen, so this amount of Fe could leave the reactor in the gas phase due to the low boiling point of $FeCl_3$ (315 ºC) [22].

Fig. 2 shows the XRD patterns of the combustion ash and gasification ash before the desulphurization tests. Species such as quartz, calcite, iron oxides and different calcium and iron phosphates were detected in the ash samples. The oxidation state of Fe is one of the main differences in the XRD patterns: Fe appears in the form of hematite (Fe_2O_3) in the combustion ash and in the form of magnetite (Fe_3O_4) in the gasification ash. Concordantly, the reddish color characteristic of hematite was only observed on the combustion ash.

3.2. Desulphurization performance: H_2S/N_2 mixture as inlet gas

Different tolerable levels of sulphur in gas products can be found in the literature depending on the gas application. For instance, the H_2S concentration limit ranges between 20 and 750 ppmv for gas turbine applications [14]. An intermediate value of 100 ppmv has been used in this work to define the H_2S breakthrough time.

The H_2S breakthrough curves obtained for the dry and moist H_2S/N_2 mixtures are depicted in Fig. 3 as a function of temperature and type of ash. A gas essentially free of H_2S was obtained during 300 min and 260 min when using the combustion ash and the gasification ash, respectively, at 800 ºC and under dry conditions (Fig. 3a). However, when steam was present in the reaction medium, the H_2S breakthrough time corresponding to the combustion ash was reduced to 50 min, while an abrupt increase in the H_2S outlet flow was observed from the beginning of the experiment when using the gasification ash (Fig. 3b). According to the general reaction of metal oxides with H_2S

(1), thermodynamics predicts a negative effect of steam on the equilibrium between H_2S and metal oxide sorbents because of the simultaneous regeneration of the spent metal sulphides:

$$Me_xO_y\ (s) + y\ H_2S\ (g) \leftrightarrow Me_xS_y\ (s) + y\ H_2O\ (g) \qquad \Delta H < 0 \qquad (1)$$

Experimental results reported in the literature show different steam impact levels depending on the sorbent and the factors affecting the sulphidation rate [15]. For instance, Kim et al. studied the effect of steam on H_2S removal by a ZnO sorbent and found that the presence of 45% steam reduced the H_2S breakthrough time by almost half at 363 ºC [23]. In general, the effect of steam on the sulphur sorbent performance is expected to be more severe at higher temperatures, but there are not many studies concerning this effect [15]. In the present work, the H_2S breakthrough time was reduced by 85% in the presence of 30% steam when testing the combustion ash at 600-800 ºC, while the gasification ash showed even higher loss in its sulphur capture capacity as a consequence of their different metallic phases. The presence of carbon in the gasification ash also seemed to slightly affect its desulphurization performance. The downward trend observed in the H_2S outlet flow at 800 ºC (Fig. 3b) could be related to the steam gasification of the carbon present in the gasification ash. Ultimate analyses of the gasification ash before and after the experiment confirm this, as the carbon content was reduced from 3.14 to 0.25 wt. %.

The presence of steam in the gas atmosphere also affected the blank run results. As is well known, susceptible alloys, especially steels, react with H_2S, forming metal sulphides as corrosion by-products. This could explain the reduced H_2S outlet flow rate in the blank runs with respect to the inlet gas, particularly at 800 ºC and under dry operating conditions (Fig. 3a). The hot metal parts in the experimental setup do not

appear to react with H_2S under wet conditions (Fig. 3b) since, as discussed above, the formation of metal sulphides from metal oxides is restricted by the presence of steam.

The amount of H_2S (mL_{STP}) removed from the gas up to the breakthrough time was calculated using data from the blank runs as a reference:

$$V_{H_2S\ \text{removed up to breakthrough time}} = V_{H_2S\ \text{blank}} - V_{H_2S\ \text{experiment}} \qquad (2)$$

where $V_{H2S\ experiment}$ is the amount of H_2S (mL_{STP}) leaving the reactor up to the H_2S breakthrough time during each experiment and $V_{H2S\ blank}$ is the amount of H_2S (mL_{STP}) leaving the reactor in the blank run during the same experimental time. These H_2S outlet volumes were calculated by integration of the area under the breakthrough curves (Fig. 3), considering only the flow rate data up to the breakthrough time. The amounts of H_2S removed from the gas up to the breakthrough time are included in Table 4. These data have been statistically evaluated by analysis of variance (Table 5). Although the presence of a significant curvature prevents the use of the linear regression model obtained from the experimental design used, the relative influence of the factors can be assessed by the coefficients shown in Table 5. The existence of curvature appears to be due to the sharp reduction of the H_2S breakthrough time when steam was present in the reaction medium. The three studied factors (temperature, H_2O/H_2S and ash type), as well as their interactions, significantly affect the amount of H_2S removed from the gas up to the breakthrough time (p-value < 0.0001). The H_2O/H_2S ratio is the most influential factor ($\beta_{H2O/H2S}$ = -17.76). The higher the presence of steam, the smaller the amount of H_2S removed from gas. The origin of the sewage sludge ash is also a key factor in the H_2S removal process ($\beta_{Ash\ type}$ = -8.91). Larger amounts of H_2S can be removed from the gas with the combustion ash than with the gasification ash, especially at the lowest temperature. For instance, 54 mL_{STP} of H_2S·were removed from the dry gas up to the breakthrough time using the combustion ash at 600 ºC, while the

gasification ash only removed 4 mL_{STP} of H_2S before reaching the breakthrough time (Table 4). Non-significant differences in the surface features of both solids were found (Table 3), so that the difference in the desulphurization performance must be related to ash composition. On the one hand, gasification ash contains some amount of carbon that could hinder the access of H_2S to the metallic centers. However, this amount of carbon (3.14 wt. %) does not appear large enough to be the only cause for the observed differences. As discussed in subsection 3.1, metal content and metallic species detected in both types of sewage sludge ash were not exactly the same as a consequence of the different reactive atmospheres in the combustion and gasification processes. As discussed above, one of the main differences in the composition of the ash samples was related to the Fe content, which was detected in the form of Fe_2O_3 in the combustion ash and as Fe_3O_4 in the gasification ash. Yoshimura et al. [24] analyzed Fe_2O_3 and Fe_3O_4 samples after sulphidation with H_2S at 400 ºC and the patterns obtained by Extended X-ray Absorption Fine Structure (EXAFS) showed that the intensity of the peak corresponding to Fe-S coordination after sulphidation of Fe_3O_4 was lower than that in the sulphided sample of Fe_2O_3, thus indicating more difficulty in sulphiding Fe_3O_4 at low temperatures. This fact, as well as the lower Fe content detected in the gasification ash, may explain the rapid saturation of the gasification ash. The difference in the desulphurization performance of both solids was reduced with increasing temperature, probably due to a significant increase in the Fe_3O_4 sulphidation reaction rate.

As the desulphurization process is based on gas-solid reactions, the sulphidation rate is expected to be controlled by chemical reaction kinetics or by mass transfer. The effect of the reaction temperature on the amount of H_2S removed from the gas up to the breakthrough time is clearly dependent on the ash type and presence of moisture in the gas ($\beta_T = 5.46$, $\beta_{T\text{-Ash type}} = 4.94$, $\beta_{T\text{-H2O/H2S}} = -5.36$). The temperature hardly affected the

removed amount of H_2S in wet operating conditions and/or when the combustion ash was used, whereas a great positive temperature impact was observed when the gasification ash was used at dry operating conditions.

In addition to the evaluation of the H_2S breakthrough curves, sulphur content in the solid samples was measured after the desulphurization tests. These results are included in Table 4. Only a few of these data are directly comparable with each other because they refer to the total amount of sulphur removed in each complete experiment and the duration of the experiments was not the same in all cases. In general, sulphur contents detected in the gasification ash samples after the experiments performed at 600 and 700 ºC were lower than those measured in the combustion ash samples, while similar sulphur contents were obtained in both solids at 800 ºC, pointing to similar sulphidation reaction rates of Fe_2O_3 and Fe_3O_4 at high temperatures. The highest sulphur loading detected in both types of ash was around 63-64 mg $S \cdot g^{-1}_{ash}$ after operating in dry conditions and at a temperature of 800 ºC during 390 min.

In order to check the sulphur mass balance, equation (3) calculates the expected sulphur content in the used ash samples, assuming that all the H_2S mass removed from the gas remains in the solid after the desulphurization test:

$$\text{Expected sulphur content (mg S} \cdot \text{g}^{-1}\text{ash)} = \frac{V_{H_2S\ \text{blank}} - V_{H_2S\ \text{experiment}}}{22.4} \cdot 32 \qquad (3)$$

where $V_{H2S\ experiment}$ is the amount of H_2S (mL_{STP}) leaving the reactor during each complete experiment, $V_{H2S\ blank}$ is the amount of H_2S (mL_{STP}) leaving the reactor during the blank run (extrapolating to the duration of the experiment where this differs), 22.4 is the volume of one ideal gas mole at STP ($mL_{STP} \cdot mmol^{-1}$) and 32 is the sulphur atomic mass ($mg \cdot mmol^{-1}$). The expected sulphur contents are included in Table 4. These calculated data are higher than the results obtained from the elemental analyzer. This suggests that other sulphur-containing gases (not detected by the micro GC) could be

formed during the desulphurization tests. Especially striking is the difference between the results obtained in experiment 4 (800 ºC and moist H_2S/N_2 mixture), for which the expected sulphur content in the solid was around 32 mg $S \cdot g^{-1}_{ash}$, while the elemental analyzer only detected 1.4 mg $S \cdot g^{-1}_{ash}$. This latter value was significantly lower than that detected at 600 ºC (21.5 mg $S \cdot g^{-1}_{ash}$), so the final sulphur loading in the solid under wet conditions was favored at low temperatures.

Fig. 4 shows the evolution of the theoretical distribution of sulphur into the main sulphur-containing species resulting from the equilibrium simulation: Fe_xS_y, CaS, H_2S, $CaSO_4$ and SO_2. As the composition of the solid evolves over time (discontinuous bed of solid and continuous feed of gas), successive simulations for small time intervals (10 min) were performed in order to obtain an approximation to the real process during 300 min. The gas input for each equilibrium calculation was the amount of gas fed during 10 min of experiment, while the solid input was the solid resulting from the previous simulation. The amount of Ca (in the form of CaO) and Fe (in the form of Fe_2O_3) present in 1 g of sewage sludge ash was the initial solid for the theoretical simulations. Successive gas-solid contact intervals of 10 min are represented in Fig. 4. As can be noted, the formation of CaS is thermodynamically favored over the formation of Fe_xS_y in the early stage of the desulphurization process. While the desulphurization process progresses, the amount of available Ca decreases and Fe_xS_y formation becomes more significant. The remaining fraction of H_2S in the gas stream increases at high temperatures (exothermic nature of the sulphidation reaction) and in the presence of steam. Besides the formation of metal sulphides, thermodynamics predicts the formation of SO_2 and $CaSO_4$ (as a result of the reaction of the formed SO_2 with CaO). The formation of both SO_2 and $CaSO_4$ is favored in the presence of steam and the temperature increase shifts the reaction to SO_2 formation. Thus, SO_2 formation may be

the reason for the observed differences in the expected and measured sulphur contents in the ash samples. Maximum sulphur loadings of 107, 103, 42 and 38 mg $S \cdot g^{-1}_{ash}$ were predicted for experiments 1, 2, 3 and 4, respectively. Experimental results were 46%, 39%, 49% and 96% lower than the theoretical results, respectively (Table 4).

Fig. 5 shows a back-scattered electron image of the ash resulting from experiment 2. Numbers in Fig. 5 indicate the points where the elemental composition was analyzed. The atomic fractions obtained by EDX in the different superficial points are shown in Table 6. As can be noted, ash presents a heterogeneous surface and the presence of C, O, Na, Mg, Al, Si, P, S, Ca, Fe and Zn is detected in different fractions. It should be noted that the points with the highest atomic percentage of S (23.8% in point 1 and 23.7% in point 7) are also those with the highest Fe content (35.9% and 25.3%, respectively), thus suggesting the formation of either iron sulphides or iron sulphates. On the other hand, S was hardly detected in other points, such as in point 4 (mainly formed by O and Si in the form of SiO_2) or in point 6 in which, despite of the high fraction of Fe (16.1%), only 0.4 atomic % S was found. In this case, as well as in points 2 and 3, the high presence of Fe is linked with a high presence of P, which indicates the presence of iron phosphates.

Fig. 6 shows the XPS spectra in S 2p region of the ash resulting from experiment 2. Several doublets can be fitted to the experimental signal, indicating different chemical states of sulphur in the ash surface. The peak located between 160 and 164 eV is indicative of S_n^{-2} (metal sulphides), but other oxidized sulphur forms have also been detected (169 eV: SO_4^{-2}).

3.3. Desulphurization performance: synthetic gasification gas as inlet gas

The H_2S breakthrough curves obtained for the dry and moist (30 vol. % H_2O) synthetic gasification gases are depicted in Fig. 7 as a function of temperature and type

of ash. The H_2S concentration in the outlet gasification gas remained below 100 ppmv for less time than in the previous case (H_2S/N_2 mixture). Unlike occurring with the H_2S/N_2 mixture, a significant H_2S flow was detected in the outlet synthetic gasification gas from almost the beginning of all the experiments (Fig. 7). In this case, the H_2S breakthrough time was longer than 20 min only by operating with the combustion ash at 600 ºC and dry conditions (165 min). This breakthrough time was in turn significantly lower than that obtained for the H_2S/N_2 mixture under the same operating conditions (260 min). Reduction of iron oxides present in sewage sludge ash may explain this observed behavior. As discussed in the literature [17,21,25], the presence of CO and H_2 in the gasification gas creates a reducing atmosphere that causes the conversion of Fe_3O_4 and Fe_2O_3 to FeO or even to Fe^0 in the temperature range of 700-1000 ºC. FeO and Fe^0 show less favorable sulphidation equilibrium, which led to a reduction in the sulphur capture capacity [25].. The temperature rise from 600 to 800 ºC was found to be detrimental for the H_2S removal capacity of the combustion ash, probably as a consequence of the higher reduction rate of Fe_2O_3 to FeO at 800 ºC (Fig. 7a). However, the H_2S removal capacity of the gasification ash improved at higher temperature. Thus, the impact of temperature on the H_2S removal from the gasification gas is the result of the competition of reduction and sulphidation reaction rates. The influence of the other factors (presence of steam and type of sludge ash) on the H_2S removal from the gasification gas was similar to the previous case.

Table 4 shows the results of the sulphur content measured in the samples after the experiments performed with the synthetic gasification gas, as well as data calculated according to the sulphur mass balance (3). Even though the longest H_2S breakthrough time was obtained for the combustion ash at 600 ºC, the highest sulphur loading was detected in the ash used at 800 ºC (46 vs. 55 mg $S \cdot g^{-1}_{ash}$ after 240 min). The different

shape of the H_2S breakthrough curves explains this result. After the desulphurization of the moist gasification gas, the highest sulphur content was found in the combustion ash operating at 600 ºC (26.8 mg $S \cdot g^{-1}_{ash}$ after 120 min). This value was slightly higher than that obtained after the desulphurization of the moist H_2S/N_2 mixture. Therefore, although the gasification gas reduced the H_2S breakthrough time, sulphur loading in the solid was not negatively affected.

Thermodynamic data obtained for the synthetic gasification gas feed are shown in Fig. 8. In this case, neither SO_2 nor $CaSO_4$ are present at equilibrium conditions since the reducing atmosphere created by the gasification gas prevents its formation. H_2S, CaS and Fe_xS_y are the main sulphur-containing species. Some authors have experimentally detected the formation of COS in the reducing environment of the gasification gas ($H_2S + CO_2 \leftrightarrow COS + H_2O$) [26], which could explain the observed differences in the expected and measured sulphur contents in the ash samples. The comparison of Figs. 4 and 8 shows a great impact of the gas atmosphere on the distribution of sulphur between CaS and Fe_xS_y. The presence of CO_2 in the gasification gas can explain this difference since this is the responsible gas for the carbonation reaction of CaO ($CaO + CO_2 \leftrightarrow CaCO_3$). Excess CO_2 shifts the reaction to the formation of $CaCO_3$, especially at low temperatures, thus limiting the formation of CaS from CaO. Maximum sulphur loadings of 85, 84, 42 and 41 mg $S \cdot g^{-1}_{ash}$ were predicted for experiments 20, 21, 22 and 23, respectively. Experimental results were 46%, 35%, 36% and 79% lower than the theoretical results, respectively (Table 4).

Besides the H_2S removal, the composition of the inlet gasification gas was modified during the desulphurization process under certain operating conditions, thus some catalytic activity could be attributed to sewage sludge ash. The evolution of the outlet concentrations of H_2, CO, CO_2 and C_2H_x when feeding the moist synthetic gasification

gas is depicted in Fig. 9. As can be noted, the use of both types of sewage sludge ash at 800 ºC led to a slight increase in the fractions of H_2 and CO_2 and a decrease in the percentage of CO with respect to the inlet gasification gas composition. This could be attributed to an enhancement of the water-gas shift reaction ($CO + H_2O \leftrightarrow CO_2 + H_2$). Fe content in sewage sludge ash may explain this catalytic activity [27]. Furthermore, the fraction of C_2H_x was slightly reduced, suggesting an enhancement of steam reforming reactions. The fraction of CH_4 (not shown in Fig. 9) was not modified in any case (4.0 vol. %). As shown in Fig. 9, the composition of the synthetic gasification gas was hardly modified during the blank runs and during the experiments performed at 600 ºC.

4. Conclusions

The use of the solid by-products of combustion and gasification of sewage sludge for high-temperature desulphurization (600-800 ºC) of different gases containing 5000 ppmv H_2S has been evaluated in this work. The best results were obtained by using the combustion ash for H_2S removal from a dry mixture of H_2S/N_2 at 800 ºC. The H_2S breakthrough time (< 100 ppmv H_2S) was around 300 min and the sulphur loading in the spent ash was 63 mg $S \cdot g^{-1}_{ash}$. The presence of 30% steam drastically reduced the H_2S breakthrough time by 85%. Thus, the use of sewage sludge ash for H_2S removal at 600-800 ºC is only suitable for dry gases cleaning. In general, the gasification ash showed worse desulphurization ability than the combustion ash. Iron content was lower in the gasification ash (116 mg $Fe \cdot g^{-1}_{ash}$) than in the combustion ash (192 mg $Fe \cdot g^{-1}_{ash}$) and different crystalline species were detected in the ash samples: Fe_2O_3 in the combustion ash and Fe_3O_4 in the gasification ash. The reducing atmosphere created by the gasification gas negatively affected the H_2S removal due to the simultaneous reduction of Fe_2O_3 and Fe_3O_4 to FeO, whose sulphur capture capacity has been proved

to be lower. H_2S was the only sulphur-containing gas analyzed during the experiments. However, thermodynamic data pointed to the possible formation of other sulphur-containing gases during the desulphurization process, such as SO_2 or COS (this latter in a very low proportion). Therefore, the analysis of the H_2S breakthrough curves alone can lead to misleading conclusions about the sulphur capture capacity of a sorbent material. In most cases, sulphur loading detected by the elemental analyzer in the spent combustion ash was 35-50% lower than the maximum thermodynamic data calculated assuming that the total content of calcium and iron in the solid was in the form of CaO and Fe_2O_3, respectively.

Acknowledgements

The authors gratefully acknowledge the financial support provided by the Spanish Ministry of Science and Technology (research project CTQ2010-20137) and the Spanish Ministry of Education (pre-doctoral grant awarded to N. Gil-Lalaguna, AP2009-3446). Authors would also like to acknowledge the use of Servicio General de Apoyo a la Investigación (SAI, Universidad de Zaragoza) and the use of the X-ray photoelectron spectrometer and the scanning electron microscope available in the Laboratorio de Microscopías Avanzadas (LMA) at Instituto de Nanociencia de Aragón (Universidad de Zaragoza).

References

[1] Rulkens W. Sewage sludge as a biomass resource for the production of energy: Overview and assessment of the various options. Energy Fuel. 2008; 22:9-15.

[2] Fytili D, Zabaniotou A. Utilization of sewage sludge in EU application of old and new methods - A review. Renew. Sust. Energ. Rev. 2008; 12:116-40.

[3] Manara P, Zabaniotou A. Towards sewage sludge based biofuels via thermochemical conversion - A review. Renew. Sust. Energ. Rev. 2012; 16:2566-82.

[4] Gil-Lalaguna N, Sánchez JL, Murillo MB, Rodríguez E, Gea G. Air-steam gasification of sewage sludge in a fluidized bed. Influence of some operating conditions. Chem. Eng. J. 2014; 248:373-82.

[5] Abu El-Rub Z, Bramer EA, Brem G. Review of catalysts for tar elimination in biomass gasification processes. Ind. Eng. Chem. Res. 2004; 43:6911-9.

[6] Yildirim O, Kiss AA, Hüser N, Leßmann K, Kenig EY. Reactive absorption in chemical process industry: a review on current activities. Chem. Eng. J. 2012; 213:371-91.

[7] Bagreev A, Bandosz TJ. On the mechanism of hydrogen sulfide removal from moist air on catalytic carbonaceous adsorbents. Ind. Eng. Chem. Res. 2005; 44:530-8.

[8] Bandosz TJ. On the adsorption/oxidation of hydrogen sulfide on activated carbons at ambient temperatures. J. Colloid. Interf. Sci. 2002; 246:1-20.

[9] Primavera A, Trovarelli A, Andreussi P, Dolcetti G. The effect of water in the low-temperature catalytic oxidation of hydrogen sulfide to sulfur over activated carbon. Appl. Catal. A-Gen. 1998; 173:185-92.

[10] Gutiérrez-Ortiz FJ, Aguilera PG, Ollero P. Biogas desulfurization by adsorption on thermally treated sewage-sludge. Sep. Purif. Technol. 2014; 123:200-13.

[11] Ros A, Montes-Morán M, Fuente E, Nevskaia DM, Martin MJ. Dried sludges and sludge-based chars for H_2S removal at low temperature: influence of sewage sludge characteristics. Environ. Sci. Technol. 2006; 40:302-9.

[12] Ansari A, Bagreev A, Bandosz TJ. Effect of adsorbent composition on H_2S removal on sewage sludge-based materials enriched with carbonaceous phase. Carbon 2005; 43:1039-48.

[13] Yuan W, Bandosz TJ. Removal of hydrogen sulfide from biogas on sludge-derived adsorbents. Fuel 2007; 86:2736-46.

[14] Meng X, Jong W, Pal R, Verkooijen AHM. In bed and downstream hot gas desulphurization during solid fuel gasification: a review. Fuel Process. Technol. 2010; 91:964-81.

[15] Cheah S, Carpenter DL, Magrini-Bair KA. Review of mid- to high- temperature sulfur sorbents for desulphurization of biomass- and coal-derived syngas. Energy Fuel 2009; 23:5291-307.

[16] Park NK, Lee DH, Lee JD, Chang WC, Ryu SO, Lee TJ. Effects of reduction of metal oxide sorbents on reactivity and physical properties during hot gas desulphurization in IGCC. Fuel 2005; 84:2158-64.

[17] Tamhankar SS, Hasatani M, Wen CY. Kinetic studies on the reactions involved in the hot gas desulfurization using a regenerable iron oxide sorbent - I: Reduction and sulfidation of iron oxide. Chem. Eng. Sci. 1981; 36:1181-91.

[18] Álvarez-Rodríguez R, Clemente-Jul C. Hot gas desulphurisation with dolomite sorbent in coal gasification. Fuel 2008; 87:3513-21.

[19] Elseviers WF, Verelst H. Transition metal oxides for hot gas desulphurization. Fuel 1999; 78:601-12.

[20] García G, Cascarosa E, Ábrego J, Gonzalo A, Sánchez JL. Use of different residues for high temperature desulphurisation of gasification gas. Chem. Eng. J. 2011; 174:644-51.

[21] Westmoreland PR, Harrison DP. Evaluation of candidate solids for high-temperature desulfurization of low-btu gases. Environ. Sci. Technol. 1976; 10:659-61.

[22] Perry RH, Green DW. Perry's Chemical Engineer's Handbook. 7th ed. New York: McGraw-Hill; 1999.

[23] Kim K, Jeon SK, Vo C, Park CS, Norbeck JM. Removal of H_2S from steam-hydrogasifier product gas by zinc oxide sorbent. Ind. Eng. Chem. Res. 2007; 46:5848-54.

[24] Yoshimura Y, Yasuda H, Sato T, Shimada H. Utilization of thermodynamic database in the systems using molybdate and iron based catalysis. Coal Sci. Technol. 1995; 24:1275-8.

[25] Tseng TK, Chang HC, Chu H, Chen HT. Hydrogen sulfide removal from coal gas by the metal-ferrite sorbents made from the heavy metal wastewater sludge. J. Hazard. Mater. 2008; 160:482-8.

[26] Hepola J, Simell P. Sulphur poisoning of nickel-based hot gas cleaning catalysts in synthetic gasification gas. I. Effect of different process parameters. Appl. Catal. B-Environ. 1997; 14:287-303.

[27] Liu QS, Zhang QC, Ma WP, He RX, Kou LJ, Mou ZJ. Progress in water-gas-shift catalyst. Prog. Chem. 2005; 17:389-98.

Table 1. Composition of the gas mixtures (dry basis).

Gas component	H_2S/N_2 mixture (vol. %)	Synthetic gasification gas (vol. %)
CO	--	10.0
CO_2	--	15.0
H_2	--	10.0
CH_4	--	4.0
C_2H_6	--	0.2
C_2H_4	--	1.5
C_2H_2	--	0.2
H_2S	0.5	0.5
N_2	99.5	58.6

Table 2. Operating conditions in the desulphurization tests.

Experiment	Origin of sewage sludge ash	Synthetic gas mixture	Temperature (ºC)	H_2O/H_2S mass ratio	Test duration (min)
1	Combustion	H_2S/N_2	600	0	300
2	Combustion	H_2S/N_2	800	0	390
3	Combustion	H_2S/N_2	600	45	120
4	Combustion	H_2S/N_2	800	45	120
5,6,7	Combustion	H_2S/N_2	700	22.5	120
8	Gasification	H_2S/N_2	600	0	120
9	Gasification	H_2S/N_2	800	0	390
10	Gasification	H_2S/N_2	600	45	120
11	Gasification	H_2S/N_2	800	45	120
12,13,14	Gasification	H_2S/N_2	700	22.5	120
15	Blank run	H_2S/N_2	600	0	120
16	Blank run	H_2S/N_2	800	0	120
17	Blank run	H_2S/N_2	600	45	120
18	Blank run	H_2S/N_2	800	45	120
19	Blank run	H_2S/N_2	700	22.5	120
20	Combustion	Gasification gas	600	0	240
21	Combustion	Gasification gas	800	0	240
22	Combustion	Gasification gas	600	45	120
23	Combustion	Gasification gas	800	45	120
24	Gasification	Gasification gas	600	0	120
25	Gasification	Gasification gas	800	0	240
26	Gasification	Gasification gas	600	45	120
27	Gasification	Gasification gas	800	45	120
28	Blank run	Gasification gas	600	0	120
29	Blank run	Gasification gas	800	0	240
30	Blank run	Gasification gas	600	45	120
31	Blank run	Gasification gas	800	45	120

Table 3. Characterization of the ash derived from sewage sludge combustion and sewage sludge gasification.

	Sewage sludge combustion ash	Sewage sludge gasification ash
Ultimate analysis		
C (wt. %)	0.15	3.14
H (wt. %)	n.d.[a]	n.d.[a]
N (wt. %)	0.28	0.77
S (wt. %)	0.46	0.41
BET surface ($m^2 \cdot g^{-1}$)	6.5	6.7
Pore volume ($cm^3 \cdot g^{-1}$)	0.02	0.02
Average pore size (nm)	12.0	10.9
Metal content ($mg \cdot g^{-1}_{ash}$)		
Al	52	61
Ca	65	84
Fe	192	116
K	14	n.a.[b]
P	63	51
Mg	17	n.a.[b]
Na	4	n.a.[b]
Si	122	n.a.[b]
Ti	4	n.a.[b]

[a] *not detected;* [b] *not analyzed*

Table 4. Desulphurization performance results: H_2S removed from the gas up to the breakthrough time and sulphur content in the solid samples after the desulphurization tests (measured and expected data).

Gas mixture	Ash type	H_2O/H_2S mass ratio	Temperature (ºC)	$V_{H2S\ removed\ to\ breakthrough\ time}$ (mL_{STP})	Sulphur content by ultimate analysis (mg $S \cdot g^{-1}_{ash}$) [a]	Expected sulphur content (mg $S \cdot g^{-1}_{ash}$)
H_2S/N_2	Sewage sludge combustion ash	0	600	54	58 ± 1	92
		0	800	54	63 ± 4	100
		45	600	7	21.5 ± 0.8	29
		45	800	9	1.4 ± 0.1	32
		22.5	700	14	20.8 ± 0.6	38
		22.5	700	12	18.8 ± 0.2	37
		22.5	700	12	16.6 ± 0.6	36
H_2S/N_2	Sewage sludge gasification ash	0	600	4	23.2 ± 0.5	27
		0	800	48	64.4 ± 0.7	100
		45	600	2	4.9 ± 0.2	7
		45	800	0	1.1 ± 0.1	8
		22.5	700	0	14.1 ± 0.5	17
		22.5	700	0	12.6 ± 0.5	18
		22.5	700	0	11.8 ± 0.4	17
Synthetic gasification gas	Sewage sludge combustion ash	0	600	36	46.4 ± 0.6	64
		0	800	1	55 ± 4	53
		45	600	4	26.8 ± 0.5	32
		45	800	1	8.5 ± 0.5	11
Synthetic gasification gas	Sewage sludge gasification ash	0	600	1	20 ± 1	19
		0	800	0	33.2 ± 0.6	31
		45	600	1	5.8 ± 0.2	11
		45	800	1	4.5 ± 0.5	8

[a] *mean value ± standard deviation*

Table 5. ANOVA results and linear regression coefficients for the amount of H_2S removed from the gas up to the breakthrough time under the H_2S/N_2 atmosphere.

	Sum of squares (SS)	**Degrees of freedom**	**p-value**	**Coefficient (β)[a]**
Model	4544.22	7	< 0.0001	---
Intercept	---	1	---	22.36 ± 1.20
T	238.71	1	< 0.0001	5.46 ± 1.20
H_2O/H_2S	2524.05	1	< 0.0001	-17.76 ± 1.20
Ash type	635.46	1	< 0.0001	-8.91 ± 1.20
T-H_2O/H_2S	230.05	1	< 0.0001	-5.36 ± 1.20
T-Ash type	195.03	1	< 0.0001	4.94 ± 1.20
H_2O/H_2S-Ash type	213.21	1	< 0.0001	5.16 ± 1.20
T-H_2O/H_2S-Ash type	277.30	1	< 0.0001	-5.89 ± 1.20
Curvature	883.20	2	< 0.0001	---
Pure error	2.67	4	---	---
Corrected total	5430.09	13	---	---
$R^2 = 0.84$ (= SS_{model} / $SS_{corrected\ total}$)				

[a] *95% confidence interval for the regression coefficients.*

Table 6. Elemental composition (SEM/EDX) on different superficial points of the ash resulting from experiment 2.

Point in Fig. 5	Elemental composition (atomic percentage)										
	C	O	Na	Mg	Al	Si	P	S	Ca	Fe	Zn
1		29.6		1.0	2.0	1.7	4.3	23.8	1.6	35.9	
2	0.8	57.9		3.4	3.7	2.4	13.3	1.1	6.6	10.6	0.3
3	2.2	45.9	0.5	1.5	5.7	9.2	11.5	8.6	6.3	8.8	
4	0.7	69.0	0.3	0.1	0.3	27.6	0.6			0.9	
5	0.9	50.7	0.3	3.3	6.2	9.3	12.2	4.6	7.0	5.6	
6	1.6	57.9		2.4	1.4	4.0	11.7	0.4	4.1	16.1	0.4
7		33.5		0.8	1.3	7.8	3.5	23.7	4.1	25.3	

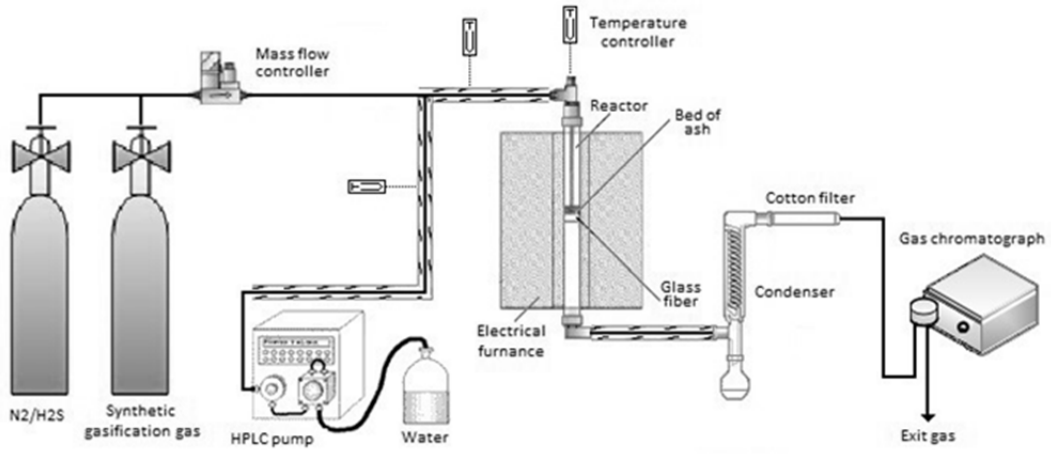

Fig.1. Experimental setup for desulphurization tests.

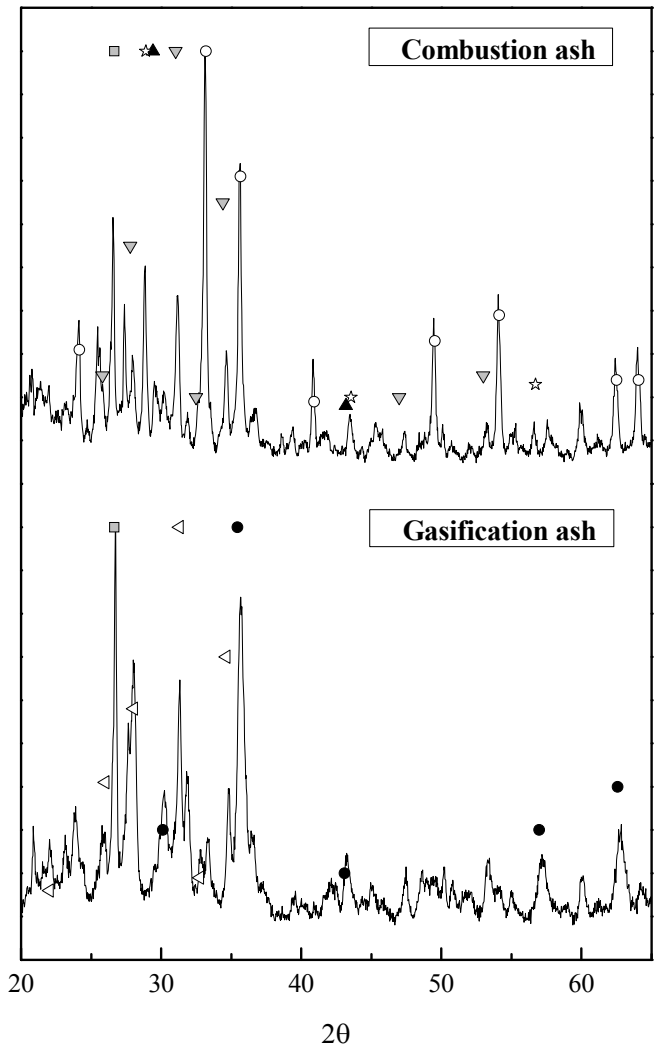

Fig. 2. XRD patterns of the fresh samples of sewage sludge combustion ash and sewage sludge gasification ash.

(a) Dry H_2S/N_2 mixture

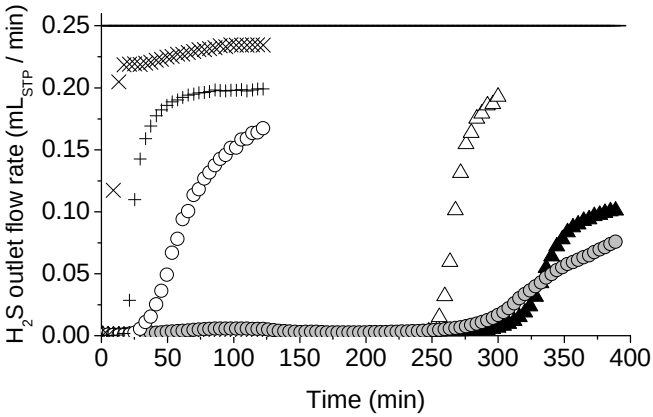

(b) Moist H_2S/N_2 mixture (30 vol. % H_2O)

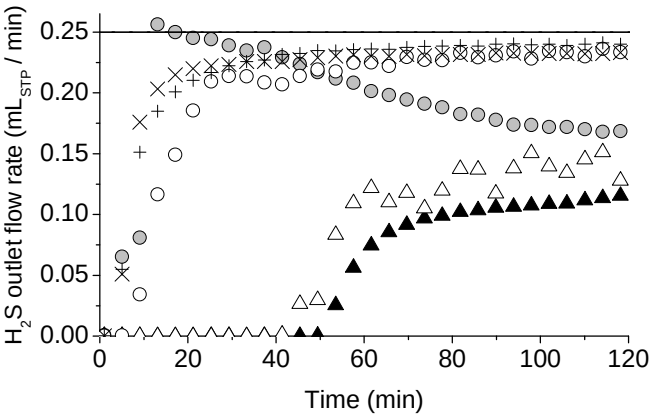

Gas feed —— ; *Blank run:* + *800 ºC,* × *600 ºC*
Sewage sludge combustion ash: ▲ *800 ºC,* △ *600 ºC*
Sewage sludge gasification ash: ● *800 ºC,* ○ *600 ºC*

Fig. 3. H_2S breakthrough curves: evolution of the H_2S flow rate ($mL_{STP} \cdot min^{-1}$) leaving the reactor when feeding the H_2S/N_2 mixture.

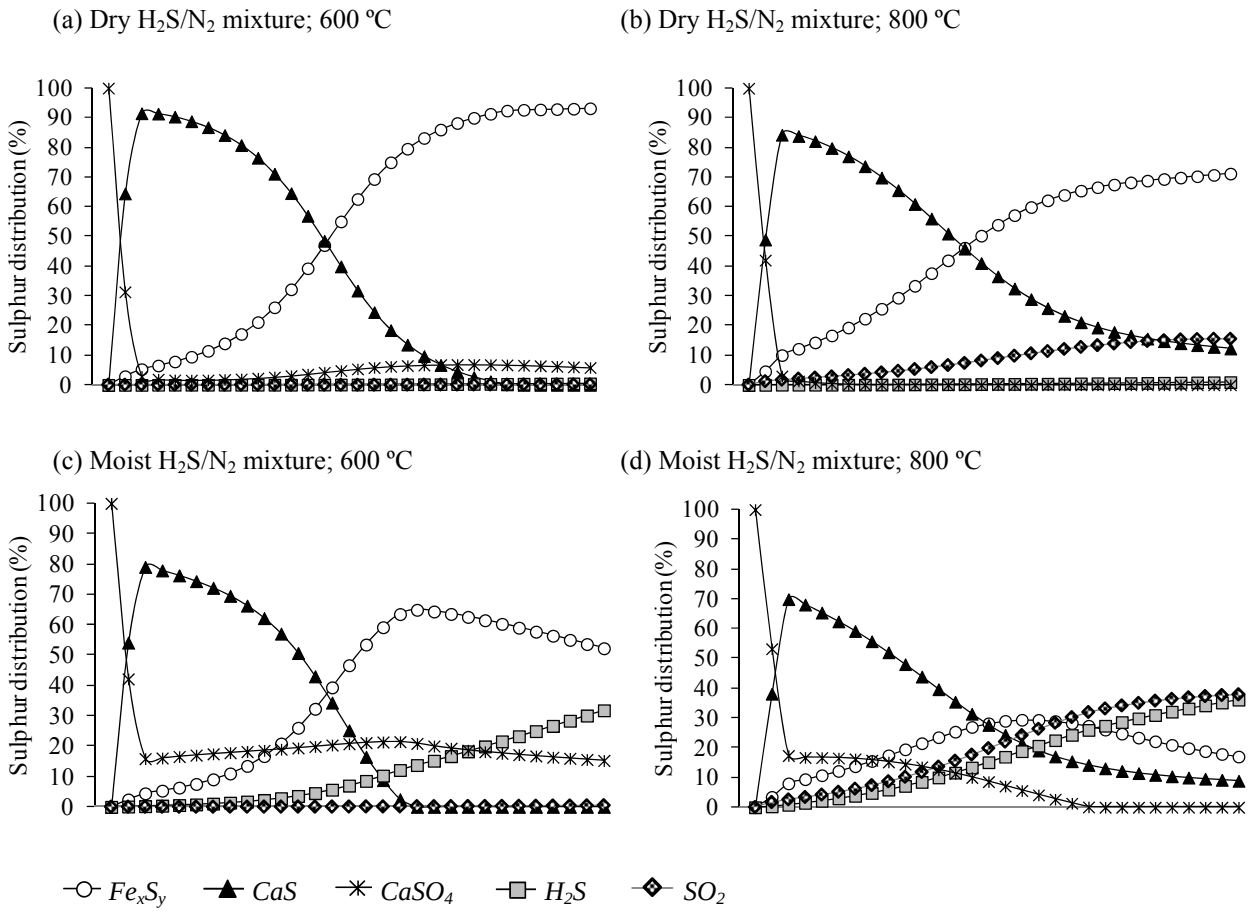

Fig.4. Evolution of the sulphur distribution into the main sulphur-containing species at equilibrium conditions (H_2S/N_2 mixture as inlet gas).

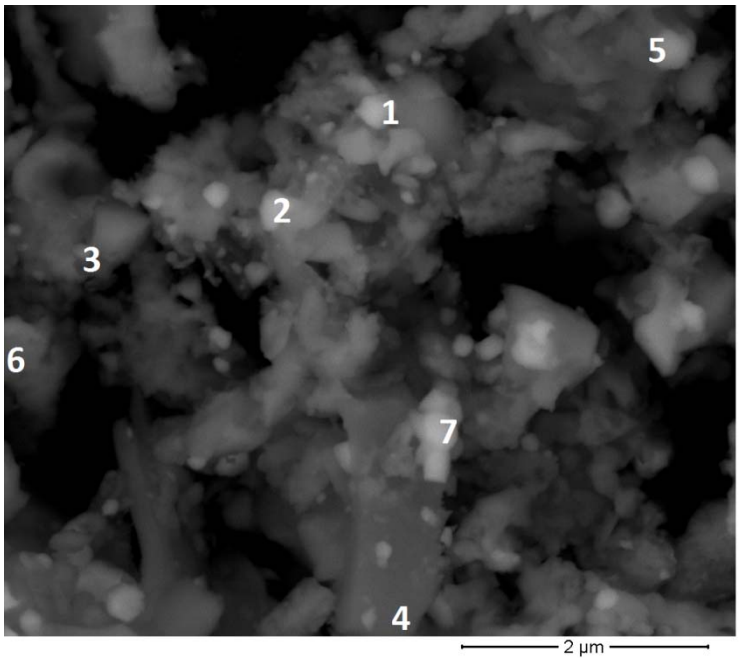

Fig. 5. Back-scattered electron image of the ash resulting from experiment 2.

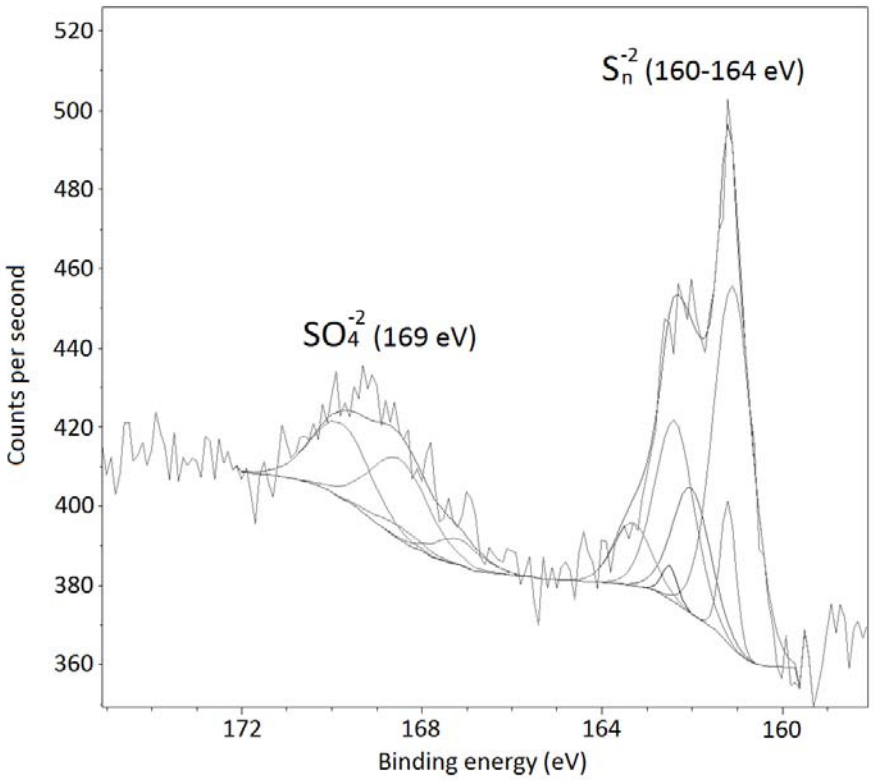

Fig. 6. XPS spectra in the S 2p region corresponding to the ash resulting from experiment 2.

(a) Dry synthetic gasification gas

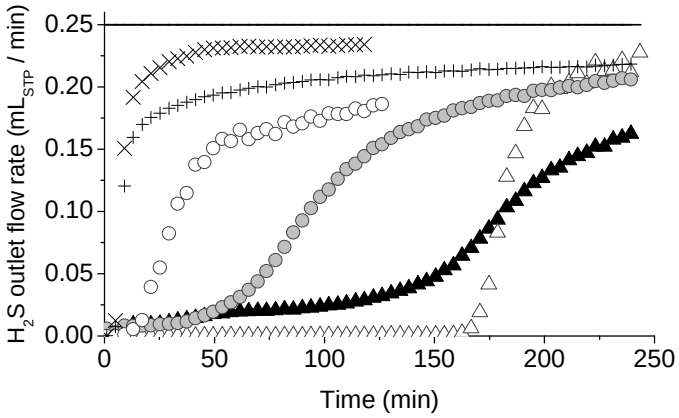

(b) Moist synthetic gasification gas (30 vol. % H_2O)

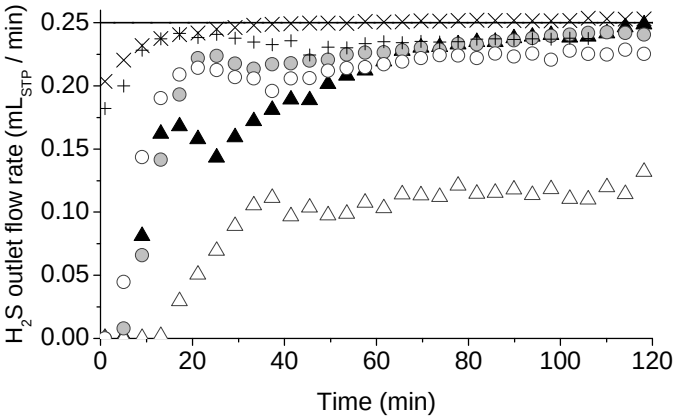

Gas feed —— ; *Blank run:* + *800 ºC,* × *600 ºC*
Sewage sludge combustion ash: ▲ *800 ºC,* △ *600 ºC*
Sewage sludge gasification ash: ● *800 ºC,* ○ *600 ºC*

Fig. 7. H_2S breakthrough curves: evolution of the H_2S flow rate ($mL_{STP} \cdot min^{-1}$) leaving the reactor when feeding the synthetic gasification gas.

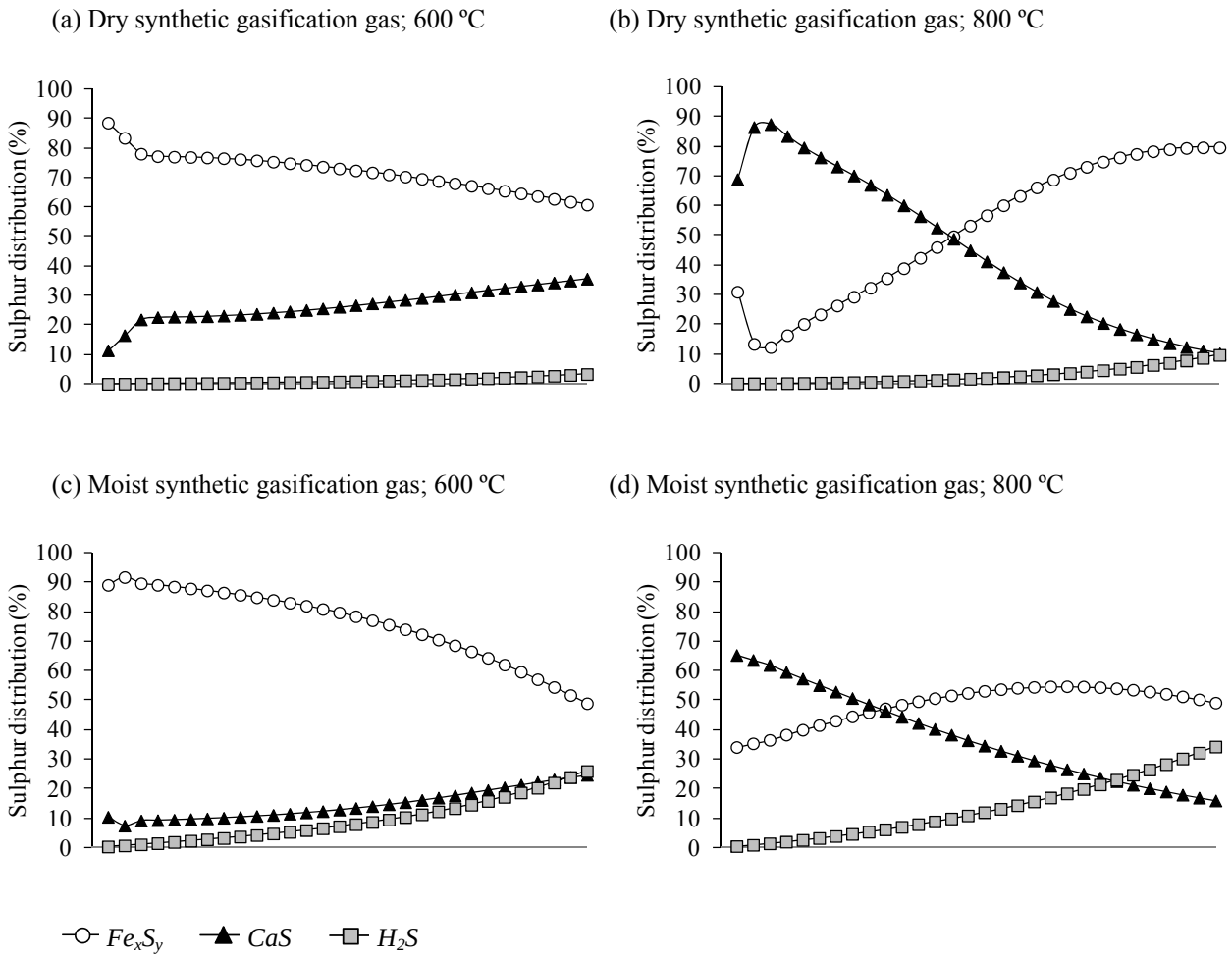

Fig. 8. Evolution of the sulphur distribution into the main sulphur-containing species at equilibrium conditions (synthetic gasification gas as inlet gas).

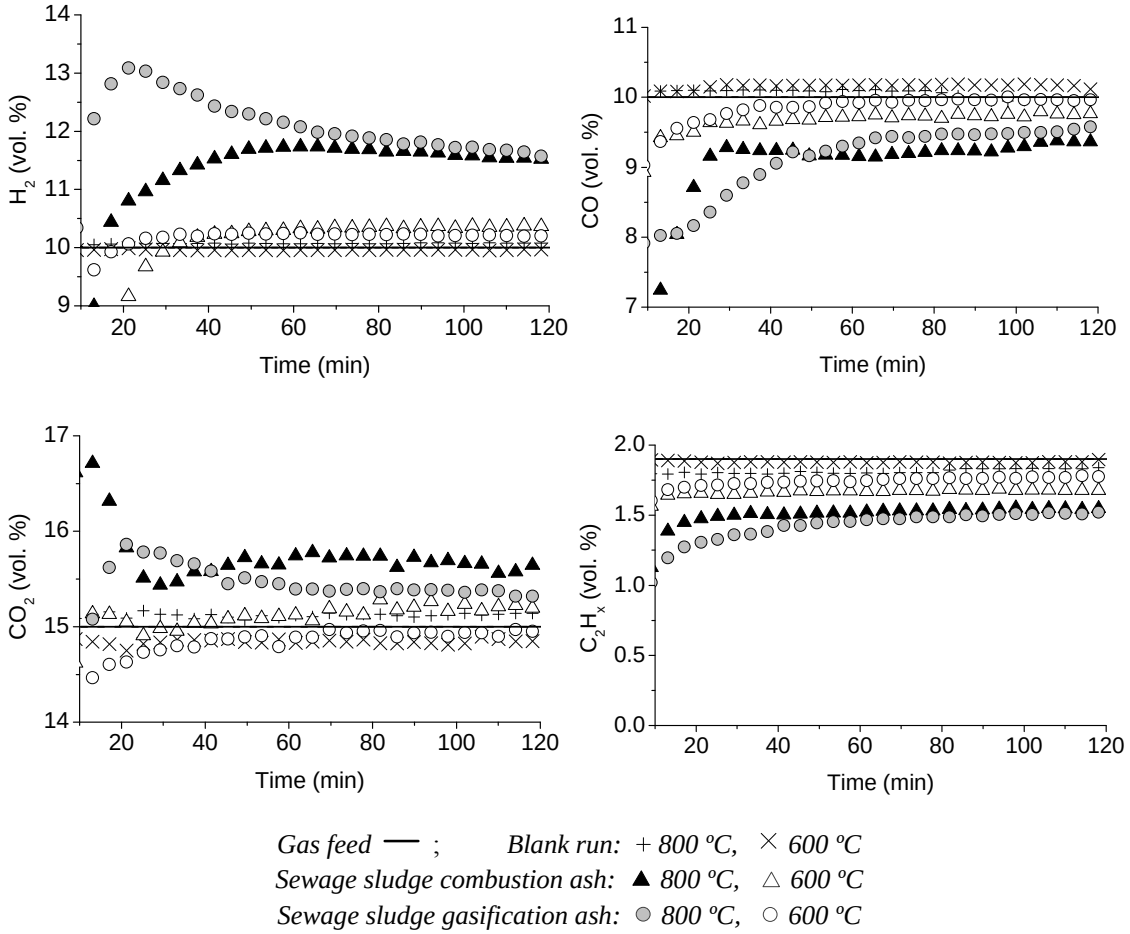

Fig. 9. Evolution of the outlet fractions of H_2, CO, CO_2 and C_2H_x (dry basis) when feeding the moist synthetic gasification gas.